RSC Advances

PAPER

View Article Online
View Journal | View Issue

Cite this: *RSC Adv.*, 2018, **8**, 35429

Photoelectric and flexible poly(styrene-*b*-ethylene/butylene-*b*-styrene)-zinc porphyrin–graphene hybrid composite: synthesis, performance, and mechanism†

Shumei Tang, Yu Xu, Gehong Su, Jianjun Bao and Aimin Zhang *

Stretchable and flexible photoelectric materials are highly desirable for the development of artificial intelligence products. However, it remains a challenge to fabricate a stable, processable, and cost-efficient material with both high photoelectric sensitivity and remarkable deformability. Herein, a new kind of photoelectric sensitive, highly stretchable and environmentally adaptive materials was developed through *in situ* synthesis and π–π conjugation design. Specifically, a photoelectric elastomer zinc porphyrin SEBS(Zn-PorSEBS) was synthesized by introducing porphyrin to SEBS chain *via* a one-pot method. Then, graphene/zinc porphyrin SEBS (G/Zn-PorSEBS) composites were obtained by combing the elastomer with graphene sheets through solution blending. Notably, the resultant flexible composites were capable of capturing light changes with illumination on or off, and the maximum photocurrent density reached 0.13 μA cm^{-2}. Moreover, the photoelectric composites exhibited a dramatic elongation (more than 1000%) and an excellent tensile strength about 20 MPa. This proposed strategy represents a general approach to manufacture photoelectric and flexible materials.

Received 21st August 2018
Accepted 1st October 2018

DOI: 10.1039/c8ra07003b

rsc.li/rsc-advances

Introduction

Organic photoelectronic materials have drawn considerable attention due to their wide applications in solar cells,[1,2] photoelectronic sensors,[3,4] and light-emitting diodes,[5,6] *etc*. Generally, good sensitivity and passable conversion efficiency are highly necessary for a desirable photoelectronic device. However, devices made from traditional photoelectronic materials are always too stiff to stretch, fold or wrinkle, which severely limits their application in flexible electronic devices such as wearable devices,[7] electronic skins,[8] and soft sensors.[9] In recent years, many strategies have been exploited to develop flexible electronics. For instance, Lai *et al.* reported a stretchable transparent electrode *via* embedding AgNWs beneath the surface of PDMS.[10–12] Lee *et al.* prepared a stretchable and patchable strain sensor based on a sandwich-like stacked nanohybrid film.[13] Li *et al.* developed a stretchable conductor by the electroless plating technique.[14] However, these materials exhibit insensitivity to light, which restricts their application in capturing light changes. Therefore, it is of great significance to develop a flexible material which is sensitive to light to cater the needs of soft photoelectronic electronics.

Poly(styrene–ethylene/butylene–styrene) (SEBS) triblock copolymer, which is synthesized through anionic polymerization and hydrogenation using styrene and butadiene as raw materials, is a kind of useful commercial thermoplastic elastomer.[15] It features in microphase separated micromorphology in which polystyrene phases with high modulus are incompatible with soft EB phases. Polystyrene hard block phase which act as a physical crosslinking impart the thermoplastic nature and polybutadiene soft block phase contribute to the high elasticity of SEBS at ambient temperatures. Owing to its soft nature, excellent ageing resistance, weather fastness, hydrolysis and moisture resistance comparing to other thermoplastic elastomers such as polyurethane (TPU) and nylon elastomers (PEBA), SEBS has been widely applied as shock absorbing materials, adhesives, sealants, coatings and cable sheath.[16] Therefore, SEBS is a promising organic optoelectronic substrate that can be used in load bearing, outdoor, corrosive and wet, *etc.* harsh conditions.

In recent years, porphyrins and its derivative have attracted great attention in materials science since it has been awarded the Nobel Prizes in Chemistry several times due to their biological functionalities.[17] Porphyrins are visible light harvesting chromophores that exhibit unique physical, chemical and biological features similar to that of natural chlorophylls. They can act as efficient electron donors in various photoinduced electron transfer processes.[18,19] This feature makes porphyrins extremely useful in combination with other electron acceptors.

State Key Laboratory of Polymer Materials Engineering of China, Polymer Research Institute of Sichuan University, Chengdu 610065, China. E-mail: zhangaimin@scu.edu.cn

† Electronic supplementary information (ESI) available. See DOI: 10.1039/c8ra07003b

Based on the interactions with electron acceptors, they could achieve the conversion of optical signal to electrical signal under external stimuli.[20,21]

In order to endow the elastomer with photoelectric sensitivity, previous researchers have proposed a method to introduce porphyrins to the polymer chains, which included four steps.[22,23] First of all, a phenyl porphyrin substituted with a reactive group on the outer ring should be synthesized. Then, the substituted porphyrin should be complexed with a metal ion. After that, the surface of the polymer material should be chemically modified to produce corresponding reactive groups. Finally, a porphyrin grafted polymer is obtained through a reaction between these two reactive groups. However, the products of substituted porphyrins are always accompanied with many homologues, and separation of the target product from these homologues with extremely similar structures requires permeation chromatography, which is quite complicated and inefficient. Moreover, the yield of the target product is also not satisfactory.

Herein, a novel and effective strategy was proposed to design a stretchable photoelectric composite. The matrix of zinc porphyrin SEBS (Zn-PorSEBS) was developed through four modification steps, including chloromethylation, hydroformylation, porphyrinization and complexation by zinc acetate. The porphyrins are synthesized *via* a one-pot method, and then dynamically grafted to the SEBS chain, which greatly simplifies the separation processes of the target substituted porphyrins. Furthermore, the graft ratio of porphyrins can be artificially controllable by adjusting the reaction time in this strategy. The resulting Zn-PorSEBS elastomer exhibited good photoelectric sensitivity and remarkable stretchability. A small amount of graphene was added *via* solution blending method, and a graphene/zinc porphyrin SEBS (G/Zn-PorSEBS) composite can be obtained. The photoelectron transfer efficiency was highly enhanced due to the strong π–π conjugation between the porphyrins and graphene. In addition, without sacrifice its excellent elasticity, the mechanical strength of the composite was significantly improved. Moreover, the composite was extremely flexible to undergo a variety of deformations such as twisting, bending, folding and curling to different shapes. This simple and efficient strategy presented in this work probably open up a new opportunity for design and scalable fabrication of flexible optoelectronic materials, which possesses the advantages of being steady, soft and easy to process. This optoelectronic material could be used to fabricate smart electronic devices such as wearable devices, artificial skins of robots and stretchable electronic sensors.

Experimental

Materials

Tri-block copolymer SEBS YH-501, with number-average molecular weight of 60 000 g mol^{-1}, was supplied by Sinopec (Yue Yang). 1,4-Bis(chloromethoxy)butane (BCMB) was synthesized according to literature.[24] Pyrrole was obtained from Aladdin and distilled under nitrogen atmosphere before use. Chloroform, xylene, stannic chloride, dimethyl sulfoxide (DMSO), sodium hydrogen carbonate, potassium iodide, lactate, benzaldehyde, ethanol and methanol were all of analytical grade and used as received from Chengdu Kelong Chemical Reagent (Chengdu).

Methods

Synthesis of chloromethylated SEBS (Cl-SEBS). In a typical synthesis, SEBS (5 g) was firstly dissolved in chloroform (230 mL). The obtained solution was cooled down to below 5 °C and then stannic chloride (4 mL) was added into the solution *via* a pipette. After that, 40 mL of BCMB-chloroform solution (50 vol%) was added dropwise to the ice-cooled chloroform solution to start the reaction. Controlling the reaction time was 1 h, 1.8 h and 2.5 h respectively, and three samples with different chloromethylation degrees were obtained. The reaction was quenched by ethanol. The chloromethylated SEBS will precipitate out immediately after adding the ethanol. The obtained products were purified by dissolution–precipitation processes for three times and then dried in a vacuum oven at 50 °C for 12 h. Unless otherwise stated, all the obtained intermediate products (*i.e.*, ALSEBS, PorSEBS, and Zn-PorSEBS) in the present study were purified according to this procedure.

Synthesis of aldehyde SEBS (ALSEBS). In a typical synthesis process, 30 mL DMSO was added dropwise to 100 mL Cl-SEBS/xylene solution (30 mg mL^{-1}) at first. Then, sodium hydrogen carbonate (1.5 g, 17.9 mmol) and potassium iodide (2.0 g, 12.0 mmol) were successively added to the mixed solution. Then the reaction mixture was refluxed at 110 °C for 6 h.

Synthesis of porphyrinated SEBS (PorSEBS). First of all, AlSEBS (1 g) and benzaldehyde (1.8 mL, 17.6 mmol) were dissolved in xylene (100 mL), and then heated to 110 °C. Afterwards, purified pyrrole (1.5 mL, 21.6 mmol) and lactic acid (2.5 mL, 33.3 mmol) were injected into the reaction mixture in sequence. The reaction was performed at 110 °C for 5 h and then quenched by ethanol.

Synthesis of zinc(II) porphyrinated SEBS (Zn-PorSEBS) elastomer. At first, Zinci acetas dihydricus (0.1 g, 0.46 mmol) was added to 100 mL PorSEBS/xylene solution (5 mg mL^{-1}). Then the solution was refluxed for 1 h and quenched *via* methanol.

Fabrication of G/Zn-PorSEBS composites. The composite films were fabricated *via* the film-casting method (Fig. 1b). Typically, 0.5 g of Zn-PorSEBS was dissolved in xylene with ultrasonic treatment at the ambient temperature. Then, a desired amount of mechanically exfoliated graphene was added to the solution. Elemental analysis and structural characterization of this graphene are shown in Fig. S1, S2 and Table S1.† The mixture was exposed to ultrasonic for 2 h. Afterward, the uniform mixture was poured into a Teflon mold and then placed in a vacuum oven (60 °C) for volatilization. After 24 hours, a flexible G/Zn-PorSEBS composites with excellent photoelectric sensitivity and stretchability can be obtained. In this work, *x*% G/Zn-PorSEBS was used to abbreviate the obtained composite. The *x*% represents the mass fraction of the graphene in the composite.

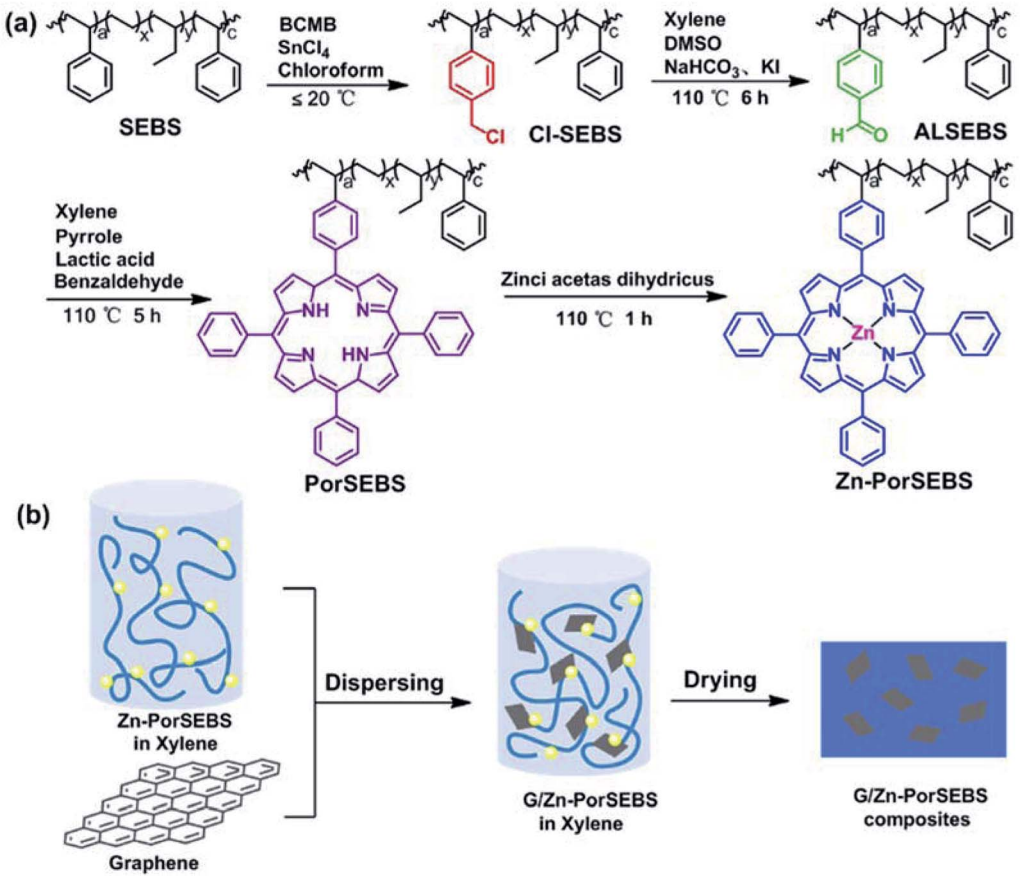

Fig. 1 (a) The synthesis processes of Zn-PorSEBS elastomer. (b) Fabrication of G/Zn-PorSEBS composites.

Characterization

The chemical structure of the SEBS precursors in each modification steps were characterized by Fourier Transform Infrared (FT-IR) spectroscopy (Nicolet iS50, USA). The ^{1}H NMR spectra of the precursors were collected on a Bruker AVANCE III-HD 600 MHz spectrometer using chloroform-d as the solvent and tetramethylsilane as the internal standard. X-ray photoelectron spectrometer (XPS, KRATOS XSAM800) with Al Kα as the X-ray source and a power of 150 W was used to determine the atomic composition in Zn-PorSEBS films. A UV3600 spectrophotometer (Shimadzu, Japan) was chosen to monitor the UV-visible absorption spectra of the samples at the wavenumber range of 200–800 nm. The electrochemical experiments were carried out with a CH Instruments Electrochemical Analyzer (model I6601). The system consisted of an indium tin oxide (ITO) working electrode, a carbon rod counter electrode, and an Ag/AgCl reference electrode. The polymer film is applied to the ITO surface by a coating method and then placed into the testing system. The electrolyte was 1 M NaOH aqueous solution. Micromorphology of gold sputtering brittle surface was observed *via* a scanning electron microscope (SEM, Quanta 250) at a voltage of 20 kV. Mechanical behavior was conducted on an Instron-5966 versatile testing machine at room temperature with an extension rate of 30 mm min^{-1}.

Results and discussion

Molecular structure analysis

The synthesis of PorSEBS mainly involves three steps. At first, the chloromethyl groups were grafted to the SEBS chains at the *para* position of benzene rings through Blanc chloromethylation.[25] Then chloromethyl groups were oxidized into aldehydes by using DMSO as the oxidants, which follows the Kornblum oxidation mechanism.[26] Finally, the obtained aldehydes were reacted with pyrrole and benzaldehyde under the catalysis of lactic acid. Thus, porphyrin rings were *in situ* synthesized at the *para* position of the benzene rings of SEBS.

FTIR spectroscopy, which is rather sensitive to the groups change can be used to confirm the chemical structure of the intermediate products in each step, as shown in Fig. 2a. In Fig. 2a, for pure SEBS, the wavenumber region of 1601–1452 cm^{-1} is assigned to the skeleton vibration of benzene rings. The peaks at 757 cm^{-1} and 698 cm^{-1} can be attributed to the monosubstituted benzene rings. The peak at 1378 cm^{-1} corresponds to the C–H bending vibration of the EB segments. It is noted that, a prominent peak at about 1265 cm^{-1} which belongs to the C–H bending vibration of CH_2–Cl groups appears after chloromethylation (Cl-SEBS),[27] indicating that the chloromethyl groups were successfully grafted on the benzene rings. However, the peak at 1265 cm^{-1} is completely absent after the

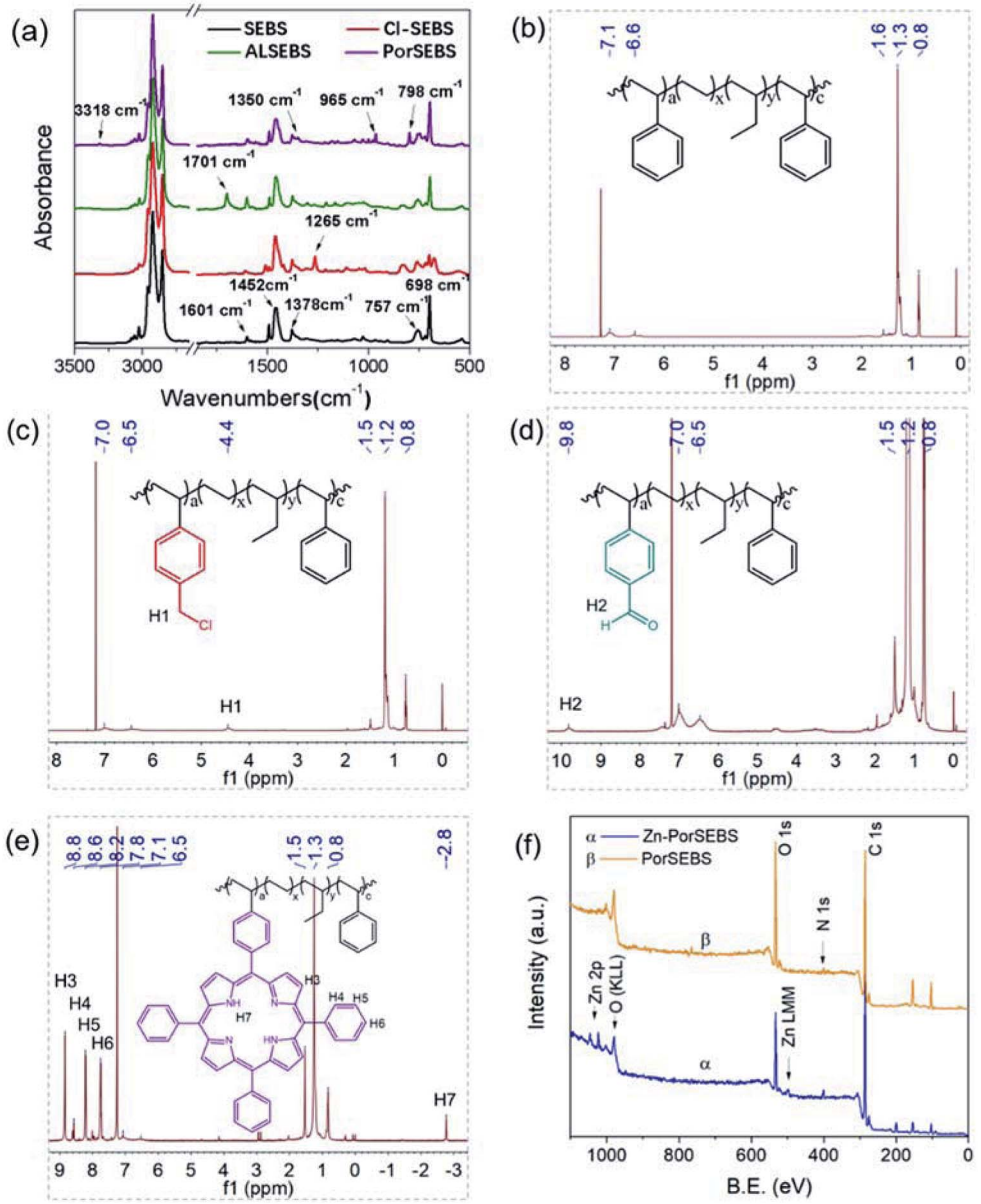

Fig. 2 (a) FT-IR spectra of SEBS, Cl-SEBS, ALSEBS and PorSEBS. (b–e) ^{1}H NMR spectra of SEBS, Cl-SEBS, ALSEBS and PorSEBS. (f) XPS spectra of PorSEBS and Zn-PorSEBS.

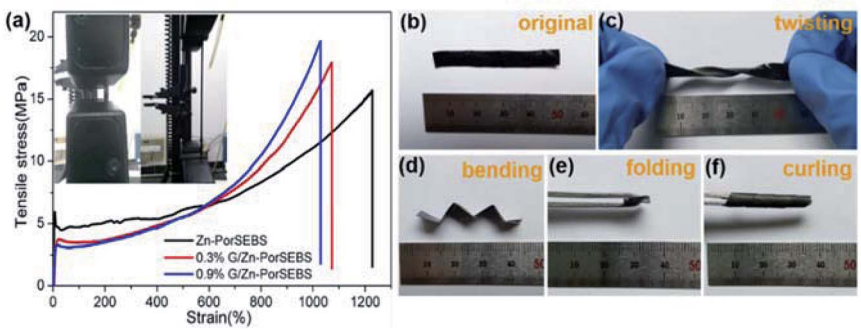

Fig. 3 (a) Typical stress–strain curves of Zn-PorSEBS and G/Zn-PorSEBS with different graphene content. Inset photos showing the high stretchability of the sample. (b–f) Pictures giving the different deformation process of G/Zn-PorSEBS composites.

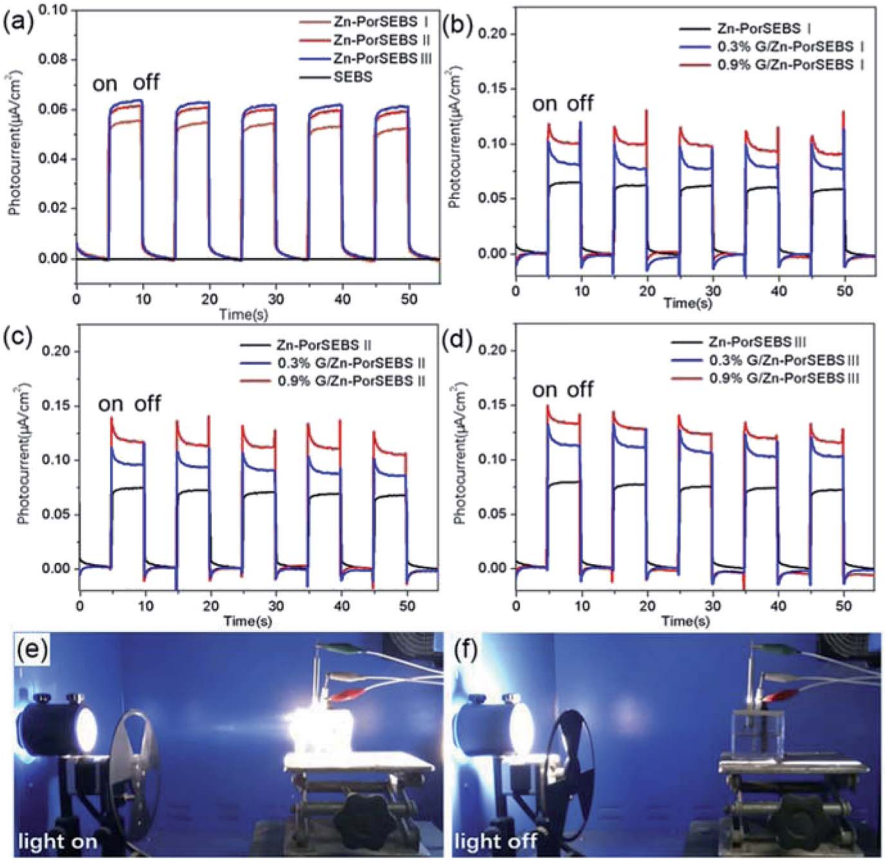

Fig. 4 Photocurrent switching response at 5 s intervals in a 0.3 V 1 M NaOH aqueous solution under 500 W Xenon lamp illumination. (a) Photocurrent response of neat SEBS and Zn-PorSEBS elastomer with different porphyrin grafting ratio. (b–d) Photocurrent response of Zn-PorSEBS elastomer and G/Zn-PorSEBS with different graphene content at the same porphyrin grafting ratio. (e and f) Photographs giving the light on/light off process.

following Kornblum reaction. Instead, a conspicuous new peak at 1701 cm^{-1} which probably belongs to the C=O stretching vibration emerges, confirming the successful synthesis of AlSEBS. At last, for PorSEBS, some new peaks located at 3310 cm^{-1} (stretching vibration of N–H groups), 1350 cm^{-1} (skeleton vibration of porphyrin ring), 965 cm^{-1} (in-plane bending vibration of N–H groups), and 798 cm^{-1} (skeleton vibration of porphyrin rings) can be clearly observed.[28] Besides, the band at 1701 cm^{-1} was completely disappeared. These changes can be attributed to the fact that the aldehyde groups on the benzene rings were replaced by porphyrin rings.

Furthermore, the ^1H NMR spectra of the intermediate products are shown in Fig. 2, which reflects their precise molecular structures. Compared to that of SEBS (Fig. 2b), the spectrum of Cl-SEBS (Fig. 2c) shows a new proton peak (H1) at 4.4 ppm, which can be attributed to the *p*-methylene protons of benzene ring.[27] After Kornblum reaction, it can be clearly seen that a new proton peak (H2) at 9.92 ppm appeared (Fig. 2d), which can be assigned to the protons of aldehyde groups in ALSEBS. In the ^1H NMR spectra of PorSEBS (Fig. 2e), the resonance signals at 8.6, 8.2 and 7.8 ppm are assigned to the *ortho*-(H4), *meta*-(H5) and *para*-protons (H6) of benzene rings in porphyrin, respectively. Typically, the resonance signals of protons in double bond (H3) and secondary amine (H7) in pyrrole rings are appear at 8.8 and −2.75 ppm, respectively.[28] All these results also clearly demonstrated that pyrrole is successfully grafted to the SEBS chains.

XPS measurement was used to confirm the complexation behavior between zinc ion and porphyrins, as shown in Fig. 2f. The peaks at 285.7 eV, 400.8 eV and 533.0 eV are shared by the full spectra of PorSEBS and Zn-PorSEBS, which correspond to C 1s, N 1s and O1s, respectively. In particular, the spectrum of Zn-PorSEBS is characterized by the peak at 494.6 eV which is assigned to Zn (LMM) and the peaks at 1031.0 eV and 1044.8 eV are corresponding to Zn 2p.[29] Furthermore, the surface content of Zn element (C_x) can be obtained from the XPS spectrum according to the peak area (A_i) and sensitivity factor (S_i) of desired element, which is expressed as $C_x = (A_x/S_x)/(\sum A_i/S_i)$. As a result, the C_x is calculated to be 0.68 wt%. The above analysis fully demonstrate that the target product Zn-PorSEBS was successfully synthesized.

Mechanical behavior

Tensile test was employed to evaluate the stretchability and elasticity of the composites. As shown in Fig. 3a, the Zn-PorSEBS elastomer exhibits a dramatic elongation (more than 1200%) and a desirable tensile strength about 15 MPa. Comparing to the Zn-PorSEBS elastomer, the G/Zn-PorSEBS composites shows

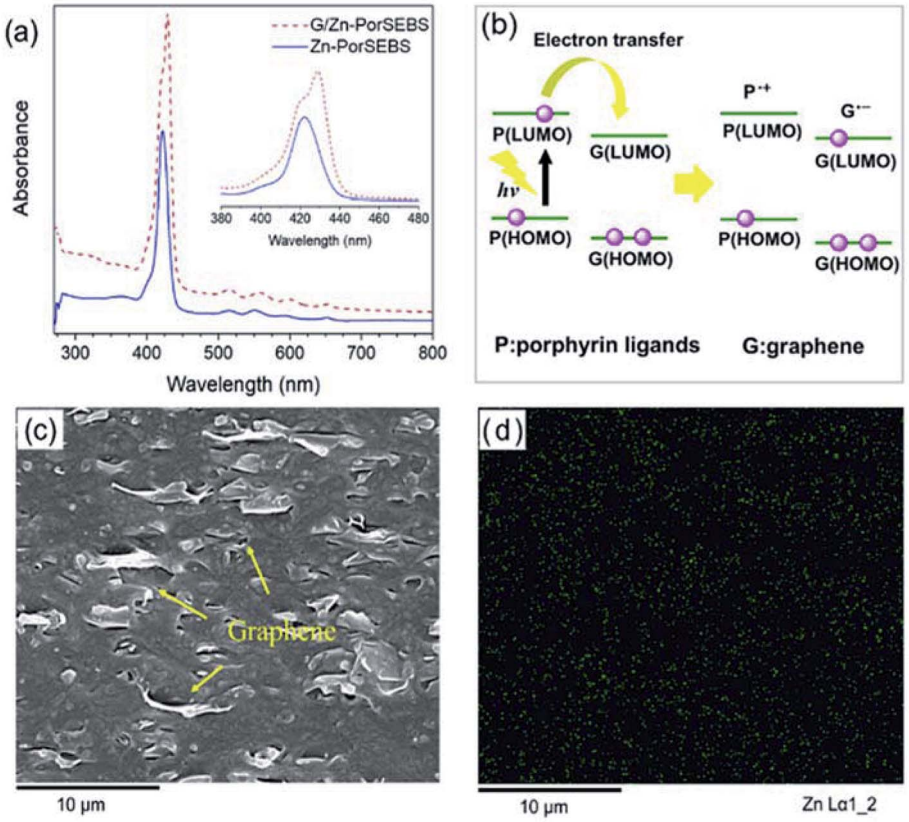

Fig. 5 (a) UV-vis spectra of Zn-PorSEBS matrix and G/Zn-PorSEBS composite. (b) Molecular orbital energy diagram of photo-induced electron transfer from porphyrin to graphene. (c) SEM and (d) EDS mapping images of G/Zn-PorSEBS composite.

a significant increase in mechanical strength but just a slight decrease in elongation. Graphene adds only 0.3 wt% and the breaking strength enhanced to 17.5 MPa. When the graphene content was added to 0.9 wt%, the breaking strength was further improved to near 20 MPa, and the elongation was still extremely high over 1000%. This is because the reinforcement due to the π–π conjugation between the porphyrins and the incorporated graphene.[30,31] As shown in Fig. 3b–f, it is worth noting that the composites are not only highly stretchable but also extremely flexible to twisting, bending, folding and curling to different shapes (Movie S1 and S2†). These results fully demonstrated that the designed photoelectric composite possesses a remarkable stretchable capability and elasticity, which is critical for its applications in flexible electronic devices.

Optoelectronic property

The photoelectric response performances of Zn-PorSEBS elastomer with different porphyrin grafting ratio and G/Zn-PorSEBS composites with different graphene content were shown in Fig. 4. Since the neat SEBS is insensitive to light, so no photocurrent can be detected (Fig. 3a). Differently from the neat SEBS, the resultant Zn-PorSEBS elastomer shows strong photoelectric response performance due to the introduction of highly photoconductive porphyrin groups. Under illumination, photon-generated excitons dissociate into free electrons and free holes, resulting in the generation of photocurrents.[32] On the contrary, if suffer from dark or insufficient light, the free electrons and free holes will be blocked by the tunnelling barrier.[33] The photoelectric response spectra shows two well-defined states, including a high-current state under illumination and a low-current state under dark, and with the light turns on and off, the two states alternate accordingly (Movie S3†).

To investigate the influence of porphyrinization degree on the photoelectric response performance of Zn-PorSEBS, three samples with different porphyrin grafting ratio were synthesized. The porphyrinization degree of Zn-PorSEBS(I), Zn-PorSEBS(II) and Zn-PorSEBS(III) were 7.2%, 10.9% and 13.6% respectively (Fig. S3–S5 and Table S2†). It was found that the photocurrent intensity of Zn-PorSEBS elastomer enhanced with increasing of the porphyrinization degree (Fig. 4a). The Zn-PorSEBS(III) elastomer achieves a highest photocurrent of about 0.06 μA cm^{-2}.

Moreover, compared to the Zn-PorSEBS elastomer, the G/Zn-PorSEBS composites are more sensitive to the incident light due to the existence of graphene (Fig. 4b–d). The photocurrent intensity of G/Zn-PorSEBS composites enhances with increasing the mass fractions of graphene. The 0.9% G/Zn-PorSEBS(III) composite shows the maximum photocurrent value of about 0.13 μA cm^{-2}, which is about 2 times larger than that of Zn-PorSEBS(III) elastomer. Previous studies indicated that this enhancement is related to the π–π interaction taking place between electron-abundant aromatic rings and

conjugated surfaces of graphene, which enables the electron transfer.[34–36]

This interaction can be captured by the UV-vis absorption spectra. As shown in Fig. 5a, Zn-PorSEBS elastomer exhibits an intense absorption band around 420 nm referred to as the Soret or B-band and four weak bands in the range of 500–700 nm named as the Q-bands, which are peculiar to the extended π electron structure of porphyrins.[37] The B-band of G/Zn-PorSEBS composite is observed at 426.6 nm, indicating a red shift existence after the incorporation of graphene, which can be attributed to the conjugation effect between graphene and Zn-PorSEBS. The Soret and Q-bands appearing in the UV-vis spectra both arise from the π–π* transitions of porphyrin ligands, which can be explained by the four frontier orbitals (HOMO and LUMO orbitals).[38,39] In Fig. 5b, an energy diagram of molecular orbitals shows the photoinduced electron transfer process from porphyrin ligands to graphene. Under irradiation of ultraviolet or visible light, porphyrins on the PorSEBS chains are excited, leading to the formation of the electrons and hole carriers.[40] Since the Fermi level of graphene is higher than Zn-PorSEBS ligands, the electrons induced by light are rapidly transferred to graphene, resulting in the electron–hole separation and thereby producing a photocurrent in an external circuit.[41] Moreover, incorporation of porphyrins light absorbing chromophores through a π–π conjugation with the highly conductive 2D graphene nanosheets would constitute an ideal donor–acceptor systems that can convert light signals to electrical signals rapidly and improve the charge-carrier mobilities and thereby mitigate the electron–hole recombination.[36,41] That's the main reason why the photocurrent intensity was remarkably enhanced when the graphene was introduced.

Beyond that, the dispersion of graphene nanosheets and zinc ions are also key factors affecting the photoelectric response properties of G/Zn-PorSEBS composites. It can be seen from the SEM image of the G/Zn-PorSEBS composite (Fig. 5c), the graphene nanosheets are uniformly embedded in the PorSEBS matrix. Besides, EDS mapping image (Fig. 5d) indicates that the zinc ions disperse homogeneously throughout the matrix phase. No agglomerations can be observed.

Conclusions

In conclusion, a facile and effective strategy is proposed for the synthesis of photoelectrical sensitive and highly stretchable elastomer. Firstly, we developed a stretchable and photoelectric sensitive elastomer by introducing the porphyrins to the SEBS chain with a controllable graft ratio through *in situ* synthesis. The obtained Zn-PorSEBS elastomer exhibited excellent photoelectricity and stretchability. Then, photoelectric composites G/Zn-PorSEBS with higher stimulated photocurrent were successfully constructed by assembling the as-prepared substrates and nanostructured conductive graphene sheets *via* π–π conjugation. Without sacrifice its outstanding elasticity of Zn-PorSEBS elastomer, the photoelectric sensitivity and tensile strength of G/Zn-PorSEBS were significantly enhanced. The obtained flexible G/Zn-PorSEBS composites can be used as photoelectric switcher to capture light changes with illumination on or off. These remarkable properties enable the designed composites to be a new generation of promising flexible photoelectric responsive materials for a range of applications such as wearable devices, electronic skin, and optoelectronic sensors.

Conflicts of interest

There are no conflicts to declare.

Acknowledgements

The authors are grateful for the financial support of the national "13th Five-Year Plan" key research and development plan (Grant no. 2017YFC1104801). The authors are grateful for the financial support of the National Key R&D Program of China (Grant no. 2017YFC1104800).

Notes and references

1 J. Hou, O. Inganäs, R. H. Friend and F. Gao, *Nat. Mater.*, 2018, **17**, 119–128.
2 B. Kan, J. Zhang, F. Liu, X. Wan, C. Li, X. Ke, Y. Wang, H. Feng, Y. Zhang, G. Long, R. H. Friend, A. A. Bakulin and Y. Chen, *Adv. Mater.*, 2018, **30**, 1704904.
3 X. Liu, S. Zhu, H. Sun, Y. Hu, S. Ma, X. Ning, L. Zhao and J. Zhuang, *ACS Appl. Mater. Interfaces*, 2018, **10**, 5061–5071.
4 O. Ostroverkhova, *Chem. Rev.*, 2016, **116**, 13279–13412.
5 Y. Liu, C. Li, Z. Ren, S. Yan and M. R. Bryce, *Nat. Rev. Mater.*, 2018, **3**, 18020.
6 B. Zhao, H. Zhang, Z. Wang, Y. Miao, Z. Wang, J. Li, H. Wang, Y. Hao and W. Li, *J. Mater. Chem. C*, 2018, **6**, 4250–4256.
7 K. Qi, J. He, H. Wang, Y. Zhou, X. You, N. Nan, W. Shao, L. Wang, B. Ding and S. Cui, *ACS Appl. Mater. Interfaces*, 2017, **9**, 42951–42960.
8 Z. Zhan, R. Lin, V. Tran, J. An, Y. Wei, H. Du, T. Tran and W. Lu, *ACS Appl. Mater. Interfaces*, 2017, **9**, 37921–37928.
9 D. Chen and Q. Pei, *Chem. Rev.*, 2017, **117**, 11239–11268.
10 T. Cheng, Y. Zhang, W. Lai and W. Huang, *Adv. Mater.*, 2015, **27**, 3349–3376.
11 D. Li, W. Lai, Y. Zhang and W. Huang, *Adv. Mater.*, 2018, **30**, 1704738.
12 T. Cheng, Y. Zhang, W. Lai, Y. Chen, W. Zeng and W. Huang, *J. Mater. Chem. C*, 2014, **2**, 10369–10376.
13 E. Roh, B. Hwang, D. Kim, B. Kim and N. Lee, *ACS Nano*, 2015, **9**, 6252–6261.
14 F. Han, X. Su, M. Huang, J. Li, Y. Zhang, S. Zhao, F. Liu, B. Zhang, Y. Wang, G. Zhang, R. Sun and C. Wong, *J. Mater. Chem. C*, 2018, **6**, 8135–8143.
15 A. D. Mohanty, C. Y. Ryu, Y. S. Kim and C. Bae, *Macromolecules*, 2015, **48**, 7085–7095.
16 D. Hofmann, R. Thomann and R. Mülhaupt, *Macromol. Mater. Eng.*, 2018, **303**, 1700324.
17 S. Ishihara, J. Labuta, W. Van Rossom, D. Ishikawa, K. Minami, J. P. Hill and K. Ariga, *Phys. Chem. Chem. Phys.*, 2014, **16**, 9713–9746.

18 S. Mathew, A. Yella, P. Gao, R. Humphry-Baker, B. F. E. Curchod, N. Ashari-Astani, I. Tavernelli, U. Rothlisberger, M. K. Nazeeruddin and M. Grätzel, *Nat. Chem.*, 2014, **6**, 242–247.
19 C. S. Diercks, S. Lin, N. Kornienko, E. A. Kapustin, E. M. Nichols, C. Zhu, Y. Zhao, C. J. Chang and O. M. Yaghi, *J. Am. Chem. Soc.*, 2018, **140**, 1116–1122.
20 C. H. A. Esteves, B. A. Iglesias, T. Ogawa, K. Araki, L. Hoehne and J. Gruber, *ACS Omega*, 2018, **3**, 6476–6482.
21 A. Rushi, K. Datta, P. Ghosh, A. Mulchandani and M. Shirsat, *Phys. Status Solidi A*, 2018, 1700956.
22 Y. Du, K. Zhu, Y. Fang, S. Zhang, X. Zhang, Y. Lu, Y. Yang, Y. Song and G. Wang, *RSC Adv.*, 2015, **5**, 48311–48322.
23 A. Wirotius, E. Ibarboure, L. Scarpantonio, M. Schappacher, N. D. McClenaghan and A. Deffieux, *Polym. Chem.*, 2013, **4**, 1903.
24 Y. Xu, S. Tang, J. Pan, J. Bao and A. Zhang, *Mater. Des.*, 2018, **146**, 1–11.
25 L. Sun, J. Guo, J. Zhou, Q. Xu, D. Chu and R. Chen, *J. Power Sources*, 2012, **202**, 70–77.
26 D. Zhang, B. Gao and K. Cui, *J. Polym. Res.*, 2016, **23**, 266.
27 M. Niu, R. Xu, P. Dai and Y. Wu, *Polymer*, 2013, **54**, 2658–2667.
28 D. Shi, R. T. Wheelhouse, D. Sun and L. H. Hurley, *J. Med. Chem.*, 2001, **44**, 4509–4523.
29 M. S. Killian, J. Gnichwitz, A. Hirsch, P. Schmuki and J. Kunze, *Langmuir*, 2010, **26**, 3531–3538.
30 X. Qi, C. Tan, J. Wei and H. Zhang, *Nanoscale*, 2013, **5**, 1440–1451.
31 X. Zhang, Y. Feng, S. Tang and W. Feng, *Carbon*, 2010, **48**, 211–216.
32 W. Hu, H. Nakashima, K. Furukawa, Y. Kashimura, K. Ajito, Y. Liu, D. Zhu and K. Torimitsu, *J. Am. Chem. Soc.*, 2005, **127**, 2804–2805.
33 M. D. Peeks, C. E. Tait, P. Neuhaus, G. M. Fischer, M. Hoffmann, R. Haver, A. Cnossen, J. R. Harmer, C. R. Timmel and H. L. Anderson, *J. Am. Chem. Soc.*, 2017, **139**, 10461–10471.
34 J. Geng, B. Kong, S. B. Yang and H. Jung, *Chem. Commun.*, 2010, **46**, 5091.
35 M. Coroș, F. Pogăcean, L. Măgerușan, M. Roșu, A. S. Porav, C. Socaci, A. Bende, R. Stefan-van Staden and S. Pruneanu, *Sens. Actuators, B*, 2018, **256**, 665–673.
36 Q. Luo, R. Ge, S. Kang, L. Qin, G. Li and X. Li, *Appl. Surf. Sci.*, 2018, **427**, 15–23.
37 M. Managa, B. Pitchou Ngoy, D. Mafukidze and T. Nyokong, *J. Lumin.*, 2018, **194**, 739–746.
38 G. de la Torre, G. Bottari, M. Sekita, A. Hausmann, D. M. Guldi and T. Torres, *Chem. Soc. Rev.*, 2013, **42**, 8049.
39 C. Hsieh, H. Lu, C. Chiu, C. Lee, S. Chuang, C. Mai, W. Yen, S. Hsu, E. W. Diau and C. Yeh, *J. Mater. Chem.*, 2010, **20**, 1127–1134.
40 K. Rybicka-Jasińska, W. Shan, K. Zawada, K. M. Kadish and D. Gryko, *J. Am. Chem. Soc.*, 2016, **138**, 15451–15458.
41 C. Ruan, L. Zhang, Y. Qin, C. Xu, X. Zhang, J. Wan, Z. Peng, J. Shi, X. Li and L. Wang, *Mater. Lett.*, 2015, **141**, 362–365.